



Cite this: *Biomater. Sci.*, 2023, **11**, 7768

# Combining biomimetic collagen/hyaluronan hydrogels with discogenic growth factors promotes mesenchymal stroma cell differentiation into Nucleus Pulposus like cells<sup>†</sup>

Prince David Okoro,<sup>‡a</sup> Antoine Frayssinet,<sup>‡a</sup> Stéphanie De Oliveira,<sup>a</sup> Léa Rouquier,<sup>b</sup> Gregor Miklosic,<sup>id c</sup> Matteo D'Este,<sup>c</sup> Esther Potier<sup>b</sup> and Christophe Hélyary<sup>id \*a</sup>

Based on stem cell injection into degenerated Nucleus Pulposus (NP), novel treatments for intervertebral disc (IVD) regeneration were disappointing because of cell leakage or inappropriate cell differentiation. In this study, we hypothesized that mesenchymal stromal cells encapsulated within injectable hydrogels possessing adequate physico-chemical properties would differentiate into NP like cells. Composite hydrogels consisting of type I collagen and tyramine-substituted hyaluronic acid (THA) were prepared to mimic the NP physico-chemical properties. Human bone marrow derived mesenchymal stromal cells (BM-MSCs) were encapsulated within hydrogels and cultivated in proliferation medium (supplemented with 10% fetal bovine serum) or differentiation medium (supplemented with GDF5 and TGFβ1) over 28 days. Unlike pure collagen, collagen/THA composite hydrogels were stable over 28 days in culture. In proliferation medium, the cell viability within pure collagen hydrogels was high, whereas that in composite and pure THA hydrogels was lower due to the weaker cell adhesion. Nonetheless, BM-MSCs proliferated in all hydrogels. In composite hydrogels, cells exhibited a rounded morphology similar to NP cells. The differentiation medium did not impact the hydrogel stability and cell morphology but negatively impacted the cell viability in pure collagen hydrogels. A high THA content within hydrogels promoted the gene expression of NP markers such as collagen II, aggrecan, SOX9 and cytokeratin 18 at day 28. The differentiation medium potentialized this effect with an earlier and higher expression of these NP markers. Taken together, these results show that the physico-chemical properties of collagen/THA composite hydrogels and GDF5/TGFβ1 act in synergy to promote the differentiation of BM-MSCs into NP like cells.

Received 18th June 2023,  
Accepted 10th October 2023

DOI: 10.1039/d3bm01025b

rs.c.li/biomaterials-science

## 1. Introduction

Lower back pain (LBP) is a leading cause of disability worldwide which has a substantial socioeconomic impact and poses a burden on healthcare.<sup>1</sup> LBP is often attributed to intervertebral disc (IVD) degeneration which leads to a variety of spinal problems such as disc herniation.<sup>2</sup> The Nucleus Pulposus (NP) is predominantly affected during the early stages of degeneration.<sup>3</sup> This centrally located tissue is highly hydrated (80% wet weight) and composed of proteoglycans and collagen II

which allow for a viscoelastic behavior that confers shock-absorbing properties within the IVD.<sup>4</sup> NP degeneration involves alterations in cell function, cell death and modification of the matrix composition, ultimately resulting in the loss of disc height and spinal instability.<sup>5,6</sup>

The standard treatments for IVD degeneration involve conservative options like medication and physical therapy. When these treatments are not efficient enough and the pain is intolerable, invasive surgeries such as spinal fusion or disc arthroplasty are required. Surgeries can have significant complications and are suspected to accelerate the degeneration of adjacent IVDs.<sup>7,8</sup> Since the 00's, several alternative treatments have emerged. Among them, cell therapy based on the injection of mesenchymal stromal cells (MSCs) within degenerated Nucleus Pulposus has been evaluated.<sup>9</sup> Unfortunately, the reported outcomes are disappointing due to cell leakage and/or incomplete cell differentiation.<sup>10</sup> Nowadays, a consensus exists on the interest in encapsulating stem cells within hydrogels. After injection, such systems should allow for better cell

<sup>a</sup>Laboratoire de Chimie de la Matière Condensée de Paris, Sorbonne Université, CNRS, UMR 7574, F-75005 Paris, France.

E-mail: christophe.helary@sorbonne-universite.fr; Tel: +33144276539

<sup>b</sup>Université Paris Cité, CNRS, INSERM, ENVA, B3OA, F-75010 Paris, France

<sup>c</sup>AO Research Institute Davos (ARI), Clavadelstrasse 8, 7270 Davos, Switzerland

<sup>†</sup>Electronic supplementary information (ESI) available. See DOI: <https://doi.org/10.1039/d3bm01025b>

<sup>‡</sup>These authors have contributed equally to this work.

retention, survival, and differentiation into NP-like cells.<sup>10–12</sup> Injectable hydrogels have been found to be optimal candidates as cell carriers due to their minimally invasive delivery method. Hydrogels can be synthesized from synthetic polymers, natural polymers or extracellular matrix (ECM) blends. Synthetic polymers are appropriate to achieve mechanical and physical properties mimicking the NP ones.<sup>13,14</sup> However, these materials lack patterns for cellular recognition. Hence, they are usually functionalized to optimize cell survival. Poly (*N*-isopropylacrylamide) (pNIPAM) has been evaluated *in vitro* to treat the degenerated NP. Encapsulated MSCs can differentiate within pNIPAM hydrogels but this polymer is not degraded by cells.<sup>15</sup> Polyethylene glycol (PEG) has been broadly used either on its own or functionalized with laminin.<sup>4,16</sup> Despite its high cytocompatibility, the degradation rate is very low, thereby slowing down the hydrogel remodeling by encapsulated cells.<sup>16,17</sup>

Some natural polymers such as fibrin, collagens and hyaluronan allow cell adhesion but they usually exhibit insufficient mechanical properties.<sup>14,18</sup> To circumvent this issue, biopolymers have to be crosslinked.<sup>4</sup>

Collagen is a major component of the natural Nucleus Pulposus extracellular matrix (ECM) as it provides a fibrillar structure. In addition, this protein is biodegradable, biocompatible and allows for cell adhesion and proliferation. This is the reason why this protein was one of the first studied for disc regeneration.<sup>19</sup> However, non-crosslinked collagen hydrogels have poor mechanical strength, high enzymatic degradation, and weak stability after cell encapsulation. To overcome these limitations, collagen is often combined with other polymers.<sup>12,20</sup> Hyaluronic acid (HA) is a non-sulfated glycosaminoglycan (GAG) that is richly present in the IVD (10% dry weight). Besides proteoglycans, HA participates in NP hydration and has therefore been broadly studied for IVD regeneration. However, HA does not form hydrogels on its own. It has to be functionalized and crosslinked *via* chemicals, enzymatic methods or photo-initiators.<sup>21</sup> Moreover, HA does not allow a high cell adhesion despite the presence of its specific cell receptors such as CD 44 and RHAMM.<sup>22,23</sup>

Combining collagen and HA to form a hybrid hydrogel allows maintaining the biological benefits of collagen while improving the hydrogel's mechanical properties. Unfortunately, these hydrogels require crosslinking with toxic chemicals such as EDC/NHS. In addition, such crosslinking inhibits collagen fibrillogenesis and the resulting structure does not mimic the natural NP topography. Fabricating composite hydrogels composed of an interpenetrating network of HA and fibrillar collagen is of great interest for IVD regeneration but difficult to obtain due to the strong collagen/HA interaction which leads to precipitation.<sup>24</sup> So, first the gelation of a biopolymer is required before integrating the second one. In this case, mechanical properties are not improved and some biopolymer leakage issues are observed.<sup>25</sup> In addition, these formulations are barely injectable.

We recently demonstrated a new method for synthesizing biomimetic collagen/HA composite hydrogels that maintains

collagen fibrils while providing mechanical strength and hydration.<sup>26</sup> This “one pot” approach is based on the co-gelation of pre-neutralized type I collagen (to trigger collagen gelling) with a 6% substituted tyramine-conjugated hyaluronic acid (THA) using horseradish peroxidase (HRP) and hydrogen peroxide (H<sub>2</sub>O<sub>2</sub>) as the crosslinker. Collagen I was used in this study because of its availability and its ability to differentiate MSCs into NP like cells.<sup>19</sup> The kinetics of gelation were tuned to generate collagen fibrils before THA gelling. We performed a systematic study to understand the impact of the THA content on the hydrogel properties. Composite hydrogels with a high THA content had mechanical properties close to those of NPs, were highly hydrated and more resistant to enzymatic degradation. Lastly, they allowed fibroblast survival and proliferation thanks to the mild conditions of fabrication *via* enzymatic THA crosslinking.<sup>26</sup>

In the current study, we hypothesized that the physico-chemical properties of the previously developed Type I collagen/THA composite hydrogels could support bone marrow derived mesenchymal stromal cell (BM-MSC) survival and differentiation into NP-like cells. To this end, we first synthesized injectable composite hydrogels that closely mimic the hydration and mechanical properties, and biochemical composition of the Nucleus Pulposus. Then, we evaluated the effect of the THA content on the cell behavior. Lastly, we explored the ability of two pro-discogenic growth factors, *i.e.* GDF5 (growth differentiation factor 5) and TGF-β1 (transforming growth factor beta1) to synergistically promote BM-MSC differentiation.

## 2. Materials and methods

### 2.1 Collagen extraction and purification

Type I collagen was extracted from the tails of Young Wistar male rats as previously described (Approval number IJM B751317 from the Ministère de l'Agriculture).<sup>27</sup> Briefly, rat tails were rinsed with 70% ethanol, placed in a safety cabinet and cut in 1 cm sections from their extremity to extract tendons. After several rinses in 1× PBS (Thermo Scientific), tendons were solubilized in 500 mM acetic acid (Carlo Erba, France) for 24 hours. Then, collagen was purified by precipitation using 0.7 M NaCl (Merck). Precipitates were dissolved in a fresh 500 mM acetic acid solution. Salt elimination and pH adjustment at 4.5 was performed by dialysis against 17 mM acetic acid. The final solution was centrifuged at 30 000g for 4 hours to remove aggregates and the supernatant was stored at 4 °C until further use. The collagen concentration was determined by hydroxyproline titration<sup>28</sup> and purity was assessed by SDS-PAGE electrophoresis (MiniProtean TGX, Biorad). Finally, the concentration was set to 8.8 mg mL<sup>-1</sup> *via* evaporation under a safety cabinet and used as collagen stock solution.

### 2.2 Hyaluronan conjugation with tyramine

Conjugation of hyaluronan (HA) (MW: 280 kDa, Contipro Biotech s.r.o, Contipro, product number: 639-80-01) with tyra-

mine was performed by the amidation reaction between HA carboxylic groups and the amine group of tyramine hydrochloride (Sigma Aldrich). Hyaluronic acid sodium salt (2 g, 5 mmol carboxylic groups) was dissolved in 200 mL of ultrapure water at a final concentration of 1% (w/v) overnight. The following day, the HA solution was warmed up to 37 °C using a thermostatic oil bath. Five mmol of 4-(4,6-dimethoxy-1,3,5-triazin-2-yl)-4-methylmorpholinium chloride (DMTMM) were added to the HA solution. Subsequently, 5 mmol of Tyr were dissolved in *ca.* 5 mL deionized H<sub>2</sub>O and added dropwise. The whole mixture was stirred at 37 °C for 24 h. Following the addition of 32 mL of a NaCl saturated solution and 30 min of stirring, the newly formed tyramine-HA conjugate (THA) was precipitated by adding dropwise 96% alcohol. After several washes in 96% alcohol, the precipitate was collected by filtration under vacuum with a Gooch filter P3 and dried at 40 °C for 48 h. Lastly, THA was dissolved in 1× PBS and its concentration was adjusted to 6% (w/v) to obtain a THA stock solution. 0.1 M silver nitrate was used to detect salt residues. Synthesized THA conjugates were characterized using UV-vis spectroscopy as previously reported.<sup>26,29</sup> The molar degree of substitution (DSmol, %) was 6%, calculated by measuring the absorbance at 275 nm of a 0.1% (w/v) THA solution in ultrapure water using a Cary 5000 UV-Vis-NIR spectrophotometer (Agilent Technologies).

### 2.3 Synthesis of collagen/THA composite hydrogels

Collagen concentration was kept constant at 0.4% (w/v) for all hydrogels and varied amounts of THA were added to obtain collagen/THA ratios – 1 : 2 and 1 : 5 with final THA concentrations of 0.8% and 2% (w/v) respectively. Pure collagen (0.4% w/v) and THA (2% w/v) hydrogels were used as controls (Fig. 1). For a 1 mL hydrogel, collagen gelling was triggered by a pH increase to 7 using 100 µL of 10×-PBS and 40 µL of 0.1 M NaOH. Additionally, THA gelling was carried out using

0.5 U mL<sup>-1</sup> HRP (horseradish peroxidase, Merck) and 0.6 mM H<sub>2</sub>O<sub>2</sub> (Merck, France). Typically, collagen/THA hydrogels were prepared in a 12 well plate by first mixing THA, HRP, 10× PBS and 0.1 M NaOH. After an hour of incubation in ice, collagen was added and THA gelling was triggered by H<sub>2</sub>O<sub>2</sub> addition. Lastly, hydrogels were placed in an incubator at 37 °C for 30 min to complete the gelation process. The different volumes to generate the different composite hydrogels are listed in ESI No. 1.†

### 2.4 Human bone marrow mesenchymal stromal cell (hBM-MSC) culture

All experiments with hBM-MSC were performed in accordance with the guidelines of Lariboisière Hospital and experiments were approved by Paris Cité University. Human BM-MSCs were isolated from bone marrow samples obtained as discarded tissue during orthopaedic surgeries at Trousseau and Lariboisière Hospital (Paris, France) following Lariboisière Hospital regulations and after patient's or parent's informed consent (4 donors, 5–22 years old, 1 female, 3 males). The cells were isolated by plastic adhesion, amplified and analyzed using flow cytometry to ensure expression of characteristic MSC markers (CD90+, CD73+, CD105+, CD45–). BM-MSCs from each donor were amplified separately in Alpha MEM Eagle (PAN-Biotech) supplemented with 10% fetal bovine serum (FBS) (Dominique Dutscher) and 1% penicillin/streptomycin (Gibco). Cells were cultivated in an incubator set to 37 °C and 5% CO<sub>2</sub> with the culture medium changed every 3 days. When reaching 85–90% confluence, BM-MSCs were used at passage 5 for 3D culture.

### 2.5 Cell encapsulation within collagen/THA composite hydrogels and 3D cell culture

Prior to their encapsulation, BM-MSCs from each donor were detached with 0.05% trypsin, counted, pooled at 1 : 4 and their final density was adjusted to 5 × 10<sup>6</sup> cells per mL. Pure and



Fig. 1 Different formulations of collagen/THA hydrogels.

composite hydrogels were prepared following the same procedure as that described in section 2.3 (Fig. 1). Working on ice, 100  $\mu\text{L}$  of cell suspension was then mixed with each forming hydrogel, just after the  $\text{H}_2\text{O}_2$  addition. The resulting cell density was about 500 000 cells per mL. The solution was dispensed in 12-well culture plates and incubated for 30 min at 37  $^\circ\text{C}$  to ensure complete gelation. Then, 2 mL of culture medium was added and hydrogels were cultivated over 28 days in an incubator set to 37  $^\circ\text{C}$  and 5%  $\text{CO}_2$ . Two different culture media were used: proliferation and differentiation media. The proliferation medium consisted of DMEM (4.5 g  $\text{L}^{-1}$  glucose with pyruvate and Glutamax) (Gibco), 10% FBS, 1% penicillin/streptomycin and 1% amphotericin B (Gibco). The differentiation medium was a serum free DMEM medium (4.5 g  $\text{L}^{-1}$  glucose with pyruvate and Glutamax) with 1% penicillin/streptomycin and 1% amphotericin B supplemented with ITS<sup>TM</sup> + Premix (Corning), 50  $\mu\text{M}$  ascorbic acid (Merck),  $10^{-8}$  M dexamethasone (Merck), 10 ng  $\text{mL}^{-1}$  human TGF- $\beta$ 1 (Peprotech) and 100 ng  $\text{mL}^{-1}$  human GDF-5 (Peprotech). Media were changed every 3 days and analysis was performed after 1, 7, 14 and 28 days.

## 2.6 Measurement of collagen/THA composite hydrogel contraction

Gross images of hydrogels were captured at each time point using a numeric camera (Kevenca) to qualitatively assess potential changes in the area due to cell contraction. These images were further analyzed using ImageJ<sup>®</sup> software to deduce the surface area of the constructs which was expressed as a percentage of the original area *i.e.*, 3.8  $\text{cm}^2$  for a 12-well plate. Six hydrogels for each condition were measured.

## 2.7 Scanning electron microscopy

Hydrogels were fixed overnight at 4  $^\circ\text{C}$  using a 4% paraformaldehyde (PFA) solution (w/v) in PBS. This step was followed by a 1 h fixation at 4  $^\circ\text{C}$  in a 2.5% glutaraldehyde solution diluted in 0.1 M cacodylate buffer pH 7.2. The samples were then dehydrated using ethanol baths with increasing concentrations up to 100% and then dried using a supercritical dryer. The samples were finally coated with a 20 nm gold layer and observed using a Hitachi S-3400N scanning electron microscope (operating at 10 kV). For each sample, images were acquired at a  $\times 10000$  magnification. Three samples per hydrogel formulation were analyzed.

## 2.8 Rheological measurements

Shear oscillatory measurements were performed on hydrogels using an Anton Paar rheometer MCR302 fitted with a 25 mm sand-blasted parallel plate upper geometry. All tests were performed at 20  $^\circ\text{C}$  with frequency sweeps. Mechanical spectra, namely storage  $G'$  and loss  $G''$  moduli *versus* frequency (0.01–10 Hz), were recorded at an imposed 1% strain, which corresponded to non-destructive conditions, as previously tested with an amplitude sweep (data not shown). In order to test all hydrogels under the same conditions, before each run, the gap between the base and geometry was chosen to apply a

slight positive normal force on hydrogels during the measurement, 0.04 N and 0.1 N. At least six samples per hydrogel formulation were tested.

## 2.9 Injectability

The different formulations were poured into a 1 mL syringe. The mixtures were injected through a 22G needle into wells of a 12 well plate. After 30 min of incubation at 37  $^\circ\text{C}$  to enable the hydrogel formation, 2 mL of culture medium was added on top of each hydrogel. Then, the mechanical properties were measured by rheometry as described in section 2.8. Cast hydrogels from the different formulations were used as controls.

## 2.10 Cell metabolic activity

Cell metabolic activity was monitored after 1, 7, 14 and 28 days of culture using the Alamar Blue assay. After 3 washes in DMEM without phenol red (Thermo Scientific), 3D cell-laden hydrogels were incubated at 37  $^\circ\text{C}$  with 300  $\mu\text{L}$  of a 10  $\mu\text{g mL}^{-1}$  resazurin solution for 5 hours. For this purpose, a stock solution of resazurin at 100  $\mu\text{g mL}^{-1}$  (Thermo Scientific) was diluted 1 in 10 in colorless DMEM culture medium. The supernatant was then collected in each well, diluted with 500  $\mu\text{L}$  of fresh colorless medium, and the absorbance was measured at  $\lambda = 570$  nm and  $\lambda = 600$  nm using a Varioskan<sup>TM</sup> LUX multi-mode microplate reader (ThermoFisher). The percentage of resazurin reduction was calculated following the instructions provided by the supplier. BM-MSCs cultured in pure collagen hydrogels at day 1 were used as controls and ascribed an arbitrary value of 100%. The results were expressed as a percentage of reduced absorbance compared to the control. Four samples per condition and time point were analyzed.

## 2.11 Cell morphology

The morphology of BM-MSCs encapsulated within collagen/THA hydrogels was observed on histological sections. Hydrogels were fixed in a 4% PFA solution (w/v) in PBS for 24 hours, then dehydrated with ethanol baths of increasing concentration (24 h in 70%, 3 h in 95% and 3 h in 100% EtOH). Afterwards, they were left in butanol for 4 days and embedded in paraffin. Seven micrometer transverse sections were prepared using a microtome (Leica). Sections were rehydrated and stained with Mayer's hematoxylin solution (Merck) for 5 min. Then, sections were rinsed with deionized  $\text{H}_2\text{O}$  and dehydrated again using ethanol and toluene. The sections were finally mounted between the glass and coverslip using an Eukitt mounting medium. Samples were imaged at  $\times 400$  magnification with a Nikon Eclipse E600 POL equipped with a Nikon DS-Ri1 camera. Three samples per condition and time point were analyzed.

## 2.12 Indirect immunodetection

Antigen retrieval was performed on rehydrated histological sections using citrate buffer (10 mM sodium citrate, 0.05% Tween 20, pH 6.0) at 95  $^\circ\text{C}$  for 20 min. After cooling, the sections were rinsed three times in PBS and incubated in blocking solu-



tion (0.05% Tween PBS, 1% bovine serum albumin, 10% horse serum) for one hour. After the addition of primary antibodies, each histological section was incubated in a moist chamber at 4 °C overnight. The monoclonal mouse anti-human collagen 2 (AbCam, product number: ab34712) was diluted 1 in 50 in blocking solution to obtain a concentration of 2 ng mL<sup>-1</sup>. Regarding the monoclonal rabbit antihuman aggrecan (Abcam, product number: ab186414), the stock solution was diluted 1 in 100 in blocking solution to obtain a 1 mg mL<sup>-1</sup> concentration. The following day, the sections were rinsed three times in PBS for 5 min. Then, the mouse and rabbit Specific HRP/DAB (ABC) detection IHC kit (AbCam) was used to reveal collagen 2 or aggrecan labelling. Briefly, a secondary antibody coupled with biotin was added, endogenous peroxidases were inhibited by H<sub>2</sub>O<sub>2</sub> addition and the Streptavidin/HRP system was used to oxidize DAB into a brown product, thereby allowing antigen detection. Negative controls were carried out following the same procedure but without incubation with the primary antibody. Sections were then counterstained with Mayer's hematoxylin solution for 30 s and then extensively washed in deionized water. The sections were finally dehydrated and mounted as previously described in section 2.10. Samples were imaged at ×100 and ×400 magnification with a Nikon Eclipse E600 POL. Three samples per condition and time point were analyzed.

### 2.13 RNA purification

Total RNA was extracted from cellularized hydrogels by homogenization in 1 mL of TRIzol® reagent (Thermo Scientific) using an ULTRA-TURRAX® homogenizer. A first centrifugation step at 5000g was conducted for 15 min to remove debris. Phase separation was then performed by adding 0.2 mL of chloroform (Gibco) and centrifuged at 10 000g for 15 min. After collection of the aqueous phase, RNA purification was carried out using an RNeasy kit (Qiagen), according to the supplier's recommended procedure. Lastly, RNA concentration and purity were determined by UV spectrophotometry using a Varioskan LUX multi-plate reader (Thermo Scientific).

### 2.14 Reverse transcription into cDNA

1 µL of random primers (200 µM) (Invitrogen) and 1 µL deoxyribonucleoside triphosphates (10 mM) (Invitrogen) were added to 10 µL RNA aliquots (around 300–500 ng). Following denaturation of the secondary structure at 65 °C and primer binding, 5× reaction buffer, dithiothreitol (0.2 M) and Moloney murine leukemia virus (M-MLV) (Invitrogen) were added. After 60 min at 37 °C and the reaction was stopped by heating at 70 °C for 10 min. The resulting cDNAs were stored at –20 °C until further use.

### 2.15 Real time PCR

Gene expression of COL2A1, ACAN, COL1A1, SOX9, IBSP, KRT18 and COL 10 was evaluated using reverse transcription quantitative PCR (RT-qPCR) in a Light Cycler 480 system (Roche). For this purpose, the Light Cycler FastStart DNA Master plus SYBR Green I kit (Roche) was used. Appropriate

primers for real time RT-PCR are listed in the ESI No. 2.† Cycling conditions were as follows: initial Taq polymerase activation at 95 °C for 5 min followed by 40 cycles, each cycle consisting of 10 s denaturation at 95 °C; 15 s annealing at 60 °C and 15 s elongation at 72 °C. Then, a melting curve was generated by increasing the temperature from 60 °C to 97 °C at a rate of 0.1 °C s<sup>-1</sup> to assess the reaction specificity. The results were analyzed using a relative quantification following the Pfaffl method.<sup>30</sup> The efficiencies of the target and reference primer pairs were measured by producing a standard curve based on the amplification of a serial dilution of cDNAs. The mRNA transcript level of each target gene was normalized with the housekeeping genes RPL13A-1 and GAPDH. Fold changes in gene expression were calculated for each target gene relative to a calibration point which is the normalized gene expression of this target gene in pure collagen hydrogels cultured in differentiation medium at day 1. The value 1 was arbitrarily given to this calibration point. Three samples precondition and per time point were analyzed.

### 2.16 Statistical analysis

All experiments were carried out at least twice, and the results were expressed as mean values + standard deviation (SD). The differences between the different formulations were analyzed for each time point using the Kruskal–Wallis test. Then, a Dunn test was used as a *post-hoc* test to determine which groups are different. A *p* value < 0.05 was considered significant.

## 3. Results

### 3.1 Collagen/THA hydrogel ultrastructure

Collagen was maintained at a concentration of 0.4% for all hydrogel formulations. Cell-laden collagen hydrogels exhibited a loose fibrillar network at day 1 characteristic of low-concentrated hydrogels (Fig. 2). As expected, their ultrastructure changed during the cell culture to become denser at day 28 due to hydrogel contraction mediated by cell activity. Indeed, acellular hydrogels did not exhibit any structural changes after 28 days in the culture medium (ESI No. 3†). A mixture of 0.4% collagen and 0.8% THA (1 : 2 ratio) results in composite hydrogels showing aggregates of collagen fibrils (Fig. 2). The latter seemed to be packed due to the presence of THA. Interestingly, these hydrogels were not modified during the cell culture experiment as similar structures were observed at day 1 and 28. The addition of 2% THA (1 : 5 ratio) changed the collagen organization at day 1. Some sheet-like morphological features reminiscent of the pure THA hydrogels were observed. However, some collagen fibrils were still visible inside these sheets at day 28. Pure THA hydrogels exhibited a characteristic sheet-like structure at day 1 and 28. Similar results obtained with the differentiation medium (GDF5 and TGFB1) did not impact the ultrastructure of hydrogels (ESI No. 4†).

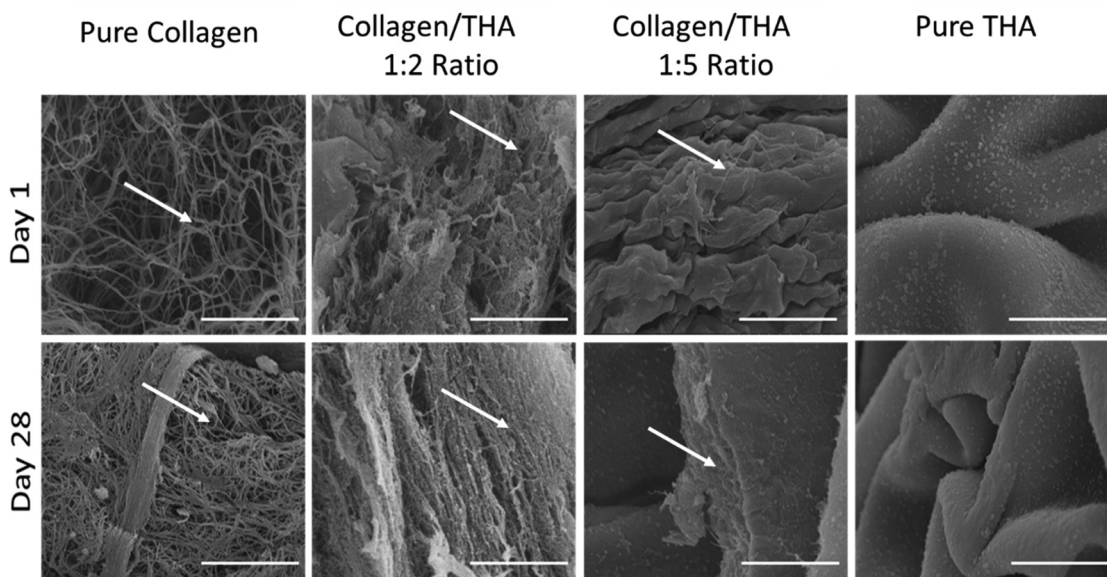


Fig. 2 Ultrastructure of cellularized collagen/THA composite hydrogels observed by scanning electron microscopy after 1 day (top) or 28 days (bottom) of culture in the proliferation medium. Hydrogel surface observed after hydrogel fracture. White arrows show collagen fibrils. Scale Bar: 5  $\mu$ m.

### 3.2 Collagen/THA composite hydrogel stability

The main parameter considered for assessing the stability of cell-laden hydrogels was the change in the surface area. With an initial area of 3.8 cm<sup>2</sup>, a potential change was monitored over 28 days for each composite hydrogel cultured in the proliferation or differentiation medium. Contraction of pure collagen hydrogels was already observed from day 1 in the proliferation medium (Fig. 3A) and the surface area progressively decreased with time to reach *ca* 10% of its original value at day 28 (Fig. 3B). The same contraction amplitude was observed in the differentiation medium (Fig. 3C). This shrinkage was likely due to BM-MSCs activities as the acellular hydrogels kept their original shape (ESI No. 5<sup>†</sup>). Composite and pure THA hydrogels did not shrink during the cell culture experiment. In contrast, a swelling phenomenon was observed proportionally to the THA content within hydrogels. For pure THA hydrogels, the surface area increased during the time course of the experiment to double at day 28. The presence of collagen within composite hydrogels showed a tendency to inhibit the swelling as the area change was about 150% and 130% for the 1 : 5 and 1 : 2 ratios, respectively (Fig. 3B and C). Again, the differentiation cell culture medium did not affect the hydrogel surface area as similar results were obtained (Fig. 3B and C).

### 3.3 Rheological properties of collagen/THA composite hydrogels

The viscoelastic properties of composite hydrogels were investigated by rheometry. For pure collagen hydrogels, a storage modulus,  $G'$ , around 100 Pa was measured at day 1. Unfortunately, the measurement was not possible from day 7 due to the extensive hydrogel contraction by cells, thereby reducing the hydrogel surface and altering its shape.

Regarding composite hydrogels,  $G'$  was slightly higher at day 1 (*ca* 150 Pa) for the 1 : 2 ratio regardless of the culture medium used (Fig. 4). For the 1 : 5 ratio, the storage modulus measured at day 1 was around 450 Pa. The latter was much higher than that measured for pure THA (around 200 Pa) at the same time point. Interestingly, the  $G'$  in these composite hydrogels was higher than the sum of moduli measured in pure collagen and THA (Fig. 4). It is worth noting that these composite hydrogels are composed of the same quantity of collagen and THA as the pure hydrogels. The storage modulus of composite and pure THA hydrogels decreased during cell culture to lose around 30% of its original value. The decrease is mainly visible between days 1 and 7. The culture medium type did not seem to impact the hydrogel mechanical properties as no significant differences were observed between the proliferation and differentiation medium (Fig. 4).

### 3.4 Injectability of collagen/THA composite hydrogels

The different hydrogel formulations were manually injected through a 22G needle as seen in the video (ESI, Video No. 3<sup>†</sup>). No significant differences were observed in storage moduli between cast and injected hydrogels (Fig. 5).

### 3.5 BM-MSC metabolic activity within collagen/THA composite hydrogels

Cell metabolic activity of BM-MSCs cultivated within pure collagen hydrogels with the proliferation medium remained quasi constant over the cell culture period (Fig. 6). Metabolic activity of BM-MSCs at day 1 was significantly lower in the composite and pure THA hydrogels with approximately 30% of the metabolic activity observed in pure collagen hydrogels. However, this value progressively increased to reach around 100% at day 28 but remained lower than that in the pure collagen hydrogel.

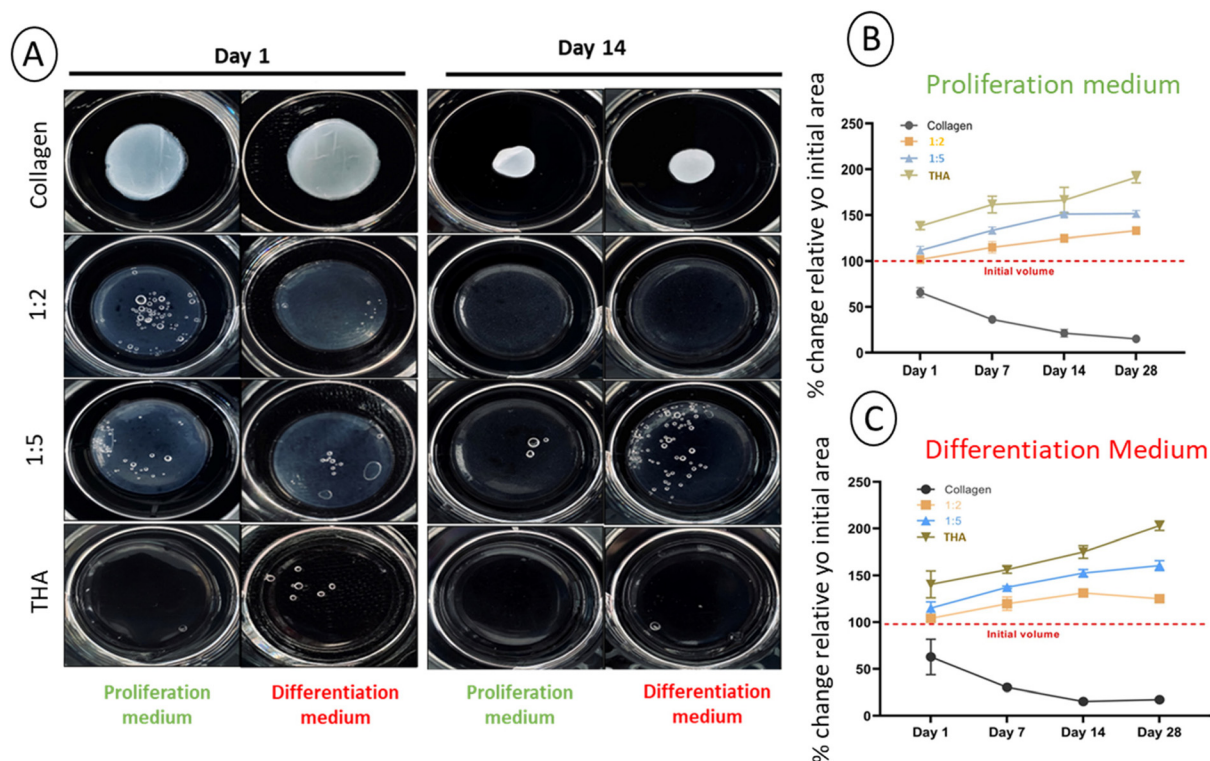


**Fig. 3** Cell-laden collagen/THA hydrogel stability. (A) Macroscopic view of collagen/THA hydrogels after one day (left) and 14 days (right) of cell culture. Changes in the surface area of the cellularized composite hydrogels cultured in proliferation (B) or differentiation medium (C) over 28 days. Results are expressed as a percentage of the initial area  $\pm$  SD ( $n = 6$ ).

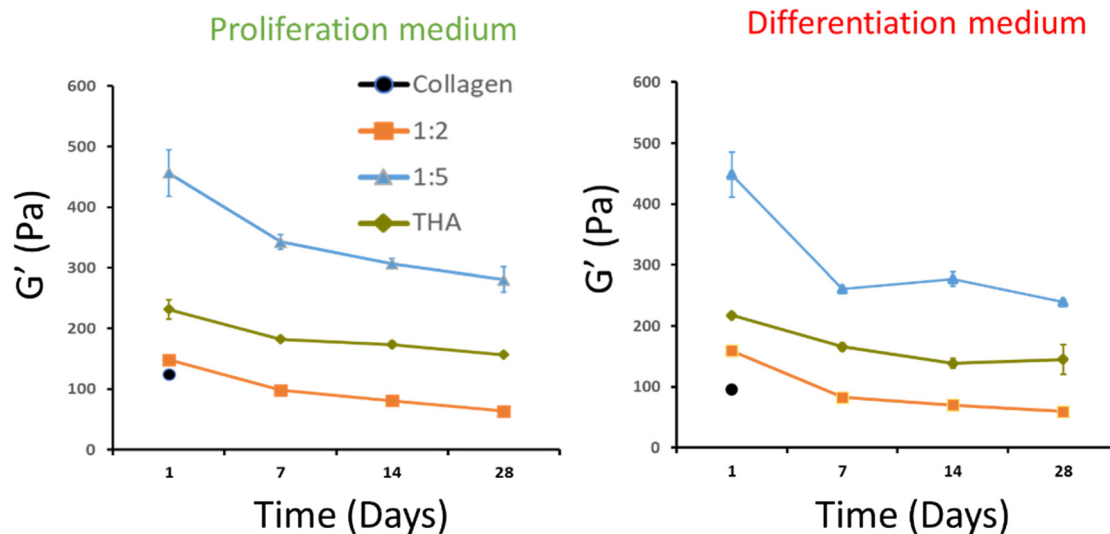


**Fig. 4** Evolution of the storage modulus of cell-laden collagen/THA composite hydrogels cultured over 28 days in the proliferation or differentiation cell culture medium. Data presented as means  $\pm$  SD for 6 biological replicates.

At day 7 and 14, the cell metabolic activity in collagen/THA hydrogels with a 1:5 ratio was significantly higher than that measured in pure THA hydrogels (Fig. 6).

In the differentiation medium, the trend was similar. At day 1, the metabolic activity of BM-MSCs within pure collagen

hydrogels was at least triple compared to the other hydrogel formulations. This cell metabolic activity was constant until day 14 but decreased by 60% at day 28. In composite and pure THA hydrogels, the cell metabolic activity increased to reach about 100% at day 28 (Fig. 6). In addition, the value measured



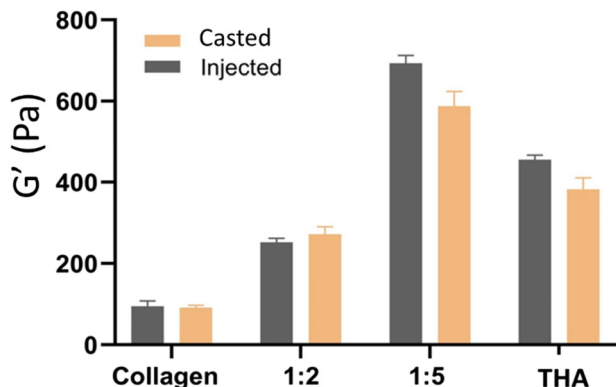


Fig. 5 Mechanical properties of cast or injected collagen/THA hydrogels ( $n = 6$ ).

in composite hydrogels with the 1:5 ratio was higher than that measured in pure THA hydrogels until day 14.

### 3.6 Cell morphology

BM-MSCs cultivated within pure collagen hydrogels exhibited a dendritic elongated shape regardless of the culture medium used (Fig. 7). When THA was added to form composite hydrogels, the cell morphology changed. Cells appeared rounded in 1:2, 1:5 and pure THA hydrogels. For the composite and pure THA hydrogels, the culture medium did not impact the cell morphology.

### 3.7 Gene expression of ECM proteins

The differentiation of BM-MSCs into NP-like cells was first investigated by their ability to express mRNA for specific ECM proteins such as collagen 2 and aggrecan. Aggrecan (ACAN) gene expression was very low in the proliferation medium at day 1 and 7 regardless of the hydrogel type. At day 14, this

gene expression increased in all hydrogels to reach *ca* 7 times the gene expression measured for the calibrator point (cells in pure collagen hydrogel culture in the differentiation medium at day 1) (Fig. 8A).

The ACAN gene expression did not increase at day 28 except for pure THA hydrogels which increased by 10 times compared to day 14 (Fig. 8A). Regarding hydrogels cultured in the differentiation medium, ACAN gene expression was detected as early as day 7 with a 2–3 fold increase in the hydrogels containing THA. This expression was correlated to the THA content at this time point. The ACAN expression then slightly increased in collagen/THA composite hydrogels at day 28 and tripled in pure THA hydrogels. In comparison to hydrogels cultured in the proliferation medium, ACAN gene expression at day 14 and 28 was not significantly different, regardless of the type of hydrogel studied.

BM-MSCs encapsulated within hydrogels weakly expressed collagen 2 until day 14 when cultured in the proliferation medium (Fig. 8B). This gene expression level remained very low for pure collagen hydrogels whereas it increased in composite and pure THA hydrogels at day 28 (Fig. 8). At this time point, COL2A1 gene expression was *ca* 10 times higher in collagen/THA composite hydrogels compared to pure collagen. In addition, the gene expression in pure THA was 10 times higher than that in composite hydrogels. Cells cultured in the differentiation medium expressed COL2A1 gene already at day 7 with an expression 100 times higher than that measured in control samples (cells in pure collagen at day 1). At this time point, COL2A1 gene expression was 10 times higher in composite and pure THA hydrogels compared to the gene expression in pure collagen hydrogels. COL2A1 gene expression increased until day 14 in all hydrogels except for the 1:2 ratio to be multiplied by 10 and 100 times for the 1:5 composite and pure THA hydrogels, respectively. It is worth noting that COL2A1 gene expression was around 100 times higher when

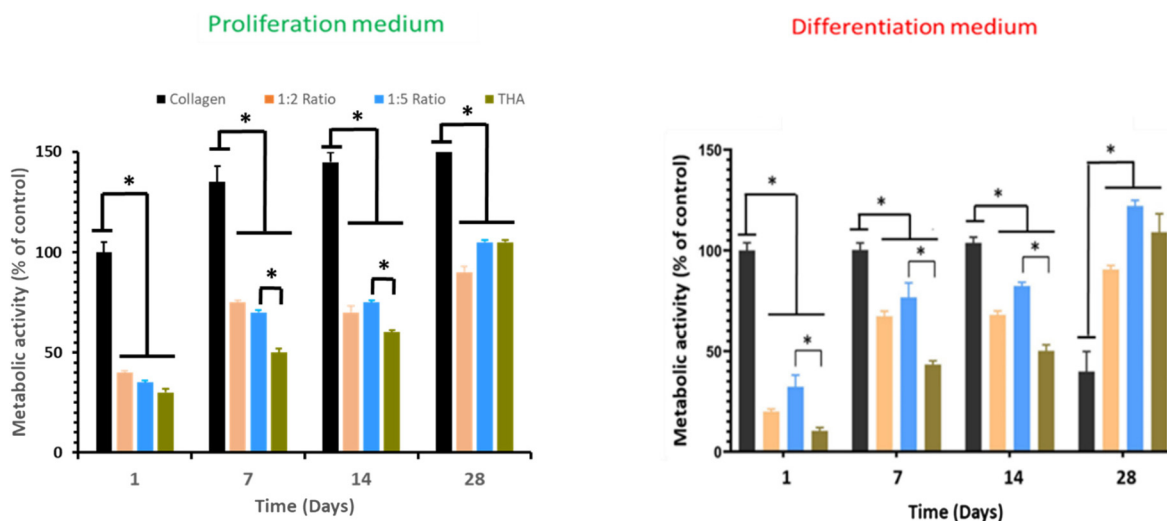


Fig. 6 Metabolic activity of human BM-MSCs within collagen/THA hydrogels cultured in the proliferation or differentiation medium over 28 days ( $n = 4$ ),  $*P < 0.05$  (Kruskal–Wallis test, *post-hoc* test: Dun).





Fig. 7 Cell morphology of BM-MSCs cultured within collagen/THA composite hydrogels in the proliferation or differentiation medium at day 14. Images obtained after Mayer's hematoxylin staining. Bar: 50  $\mu$ m.

BM-MSCs were cultivated in the differentiation medium compared to the culture in the proliferation medium (Fig. 8B).

The collagen 1 (COL1A1) gene expression, an osteoblast and fibroblast marker, was very low in all hydrogels and seemed to be inhibited by the THA content when cultured in the proliferation medium (Fig. 8C). Compared to pure collagen hydrogels, COL1A1 gene expression in composite and pure THA hydrogels was at least 5 times lower until day 14 (Fig. 8C). The differentiation medium had a positive impact on the COL1A1 gene expression in all hydrogels. However, the THA content seems to downregulate the COL1A gene expression (Fig. 8C). This expression decreased in all types of hydrogels at day 28 to reach the level observed for BM-MSCs cultured in the proliferation medium.

### 3.8 BM-MSC protein expression for NP constituents

BM-MSCs encapsulated in pure collagen hydrogels exhibited a weak collagen 2 labelling at day 14 when they were cultured in the proliferation medium (Fig. 9). The THA content within composite and pure THA hydrogels had a positive effect on collagen 2 production as the labelling appeared darker under these conditions. When cultured in the differentiation medium, collagen 2 immunodetection was stronger in all hydrogels (Fig. 9). The labelling also had a higher intensity in cells encapsulated within hydrogels containing THA (composite and pure THA) without any difference between the different conditions.

The immunodetection of aggrecan was weak in BM-MSCs cultivated in pure collagen hydrogels at day 14 (Fig. 9). In contrast, the cells exhibited a strong labelling in composite and pure THA hydrogels. No difference was visible between different hydrogels which contain THA. Additionally, the type of culture medium

used did not seem to affect the production of aggrecan, as the images for both media appeared similar (Fig. 9).

### 3.9 BM-MSC gene expression of differentiation markers

SOX 9, a major chondrogenic and NP marker, was expressed in BM-MSCs cultivated in pure collagen hydrogels in the presence of the proliferation medium. This expression was constant over 28 days. The presence of THA within hydrogels led to a weak expression of SOX 9 by cells until day 14. At day 28, SOX 9 gene expression increased in composite hydrogels and was proportional to the THA content (Fig. 10A). BM-MSCs cultivated in pure collagen hydrogel with the differentiation medium strongly expressed SOX 9 at day 7 and 14, *i.e.* around 6 times the SOX 9 expression at day 1. Afterwards, SOX 9 expression decreased and returned to its basal level at day 28. Cells cultured within composite and pure THA hydrogels had a similar trend with relatively lower gene expression of SOX 9 compared to pure collagen hydrogels, except for day 14.

Regardless of the type of hydrogel analyzed, BM-MSCs cultured in the proliferation medium did not express COL10 (collagen 10), which is the main marker of hypertrophic chondrocytes (Fig. 10B). Cells in pure collagen hydrogels, however, highly expressed collagen 10 during their culture in the differentiation medium (Fig. 10B). This expression increased until day 14 to reach 5 times its basal value. Interestingly, the presence of THA within hydrogels decreased the COL10 gene expression at least by 10 (Fig. 10B).

Integrin-binding sialoprotein (IBSP) is an osteoblast marker but also a positive marker of mature chondrocytes. It is considered to be a negative marker of NP cell differentiation. IBSP gene expression increased in BM-MSCs cultivated in the proliferation medium until day 7 (Fig. 10C). Compared to pure



**Fig. 8** Gene expression of aggrecan (ACAN), collagen 2 (COL2A1) and collagen 1 (COL1A1) of human BM-MSCs within composite hydrogels. ( $n = 3$ ). Fold change relative to the calibrator point (gene expression within pure collagen hydrogels at day 1 in the proliferation medium).  $*P < 0.05$  (Kruskal–Wallis test, *post-hoc* test: Dun).

collagen, this gene expression was slightly higher in composite and pure THA hydrogels at day 7, similar at day 14 and lower at day 28. In the differentiation medium, IBSP expression measured in pure collagen hydrogels increased to reach 20

times its basal level at day 14. In contrast, this gene expression was low in composite and pure THA hydrogels during the cell culture (10–100 times less) (Fig. 10C). Compared to the proliferation medium, IBSP was significantly less expressed in the



Fig. 9 Collagen 2 and aggrecan protein expression of BM-MSCs cultured within collagen/THA composite hydrogels at day 14.

differentiation medium for the composite and THA hydrogels but not for pure collagen hydrogels.

Cytokeratin 18 (KRT18) is a specific marker of healthy NP cells. Its gene expression increased until day 14 (Fig. 10D) for BM-MSCs cultivated in the proliferation medium. THA had a positive effect on KRT18 expression as the levels in composite and pure THA hydrogels were at least 5 times higher than those observed in pure collagen hydrogels (Fig. 10D). KRT 18 gene expression in the differentiation medium was much lower compared to cells cultivated in the proliferation medium until day 14 and were similar at day 28. At this time point, the THA content seems to have a positive impact on KRT 18 expression.

## 4. Discussion

In this study, we analyzed the impact of the physical and biochemical properties of injectable collagen/THA composite hydrogels on the differentiation of human BM-MSCs into NP-like cells. To achieve this, we modulated the THA content in the hydrogels, tailoring the mechanical properties, hydration, biochemical cues and the fibrillar collagen structure to closely

resemble the Nucleus Pulposus. Additionally, we evaluated the potential of pro discogenic growth factors, namely TGF $\beta$ 1 and GDF5, to potentialize the effects of biomimetic collagen/THA hydrogels.<sup>32,33</sup> These growth factors were used in combination to avoid the chondrocyte differentiation triggered by TGF $\beta$ 1 when used on its own and added in the culture medium at a concentration known to differentiate stem cells into NP-like cells in 2D culture.<sup>32</sup>

Synthesizing collagen/THA composite hydrogels is challenging as these biopolymers strongly interact in solution to form polyionic complexes (PICs) which precipitate.<sup>24</sup> To prevent the PICs formation and obtain a homogeneous hydrogel, hyaluronan and collagen are usually used in neutral solutions and crosslinked to form a hybrid network.<sup>34</sup> Under these conditions, fibrillogenesis is inhibited. In the present study, our strategy was to simultaneously gel collagen and THA by a pH increase and utilize HRP and H<sub>2</sub>O<sub>2</sub>. The gelling kinetics of both polymers was tuned to allow for collagen fibrillogenesis before THA crosslinking without PIC formation.<sup>26</sup> The presence of fibrils is crucial to mimic the native form of NP tissue and its specific topography.<sup>35</sup> Moreover, it has been shown that the collagen topography in the form of fibers promoted the MSCs' proliferation and differentiation.<sup>36</sup>



**Fig. 10** Gene expression of (A) SOX 9, (B) collagen 10 (COL10), (C) integrin binding sialoprotein (IBSP) and (D) cytokeratin 18 (KRT18) within collagen/THA composite hydrogels. ( $n = 3$ ). Fold change relative to the calibrator point (gene expression within pure collagen hydrogels at day 1 in the proliferation medium). \* $P < 0.05$  (Kruskal–Wallis test, *post-hoc* test: Dun).

With the aim of promoting NP regeneration, hydrogels have to be injectable and stable enough *in situ* to act as a temporary scaffold for cells. Regardless of their composition, pure and composite hydrogels developed in the present study were

injectable and their mechanical properties were not altered by the injection. Nevertheless, these hydrogels did not exhibit the same stability after gelling. The BM-MSC encapsulation within pure collagen hydrogels led to an extensive contraction of the



collagen network as described by other groups.<sup>37</sup> Hence, cell-laden collagen hydrogels do not seem to be promising biomaterials for NP regeneration. In contrast, pure THA and collagen/THA composite hydrogels swelled during the cell culture experiment. This swelling suggests that MSCs remodeled their environment, possibly by breaking some chains or cross-linking points.<sup>38</sup> In collagen/THA composite hydrogels, collagen stabilizes the structure because the swelling is smaller for 1 : 2 than for 1 : 5 hydrogels. Hence, the combination of collagen with THA seems to be the best compromise for the long-term stability of the scaffold. As previously seen, the degree of hydration is higher than 80% for composite and pure THA hydrogels.<sup>26</sup> The observed swelling is correlated to a decrease of mechanical properties at day 7. This is logical as the stiffness depends on the number of crosslinking points. For pure collagen, contraction stiffened hydrogels, leading to a decreased O<sub>2</sub> and nutrient diffusion<sup>39,40</sup> As THA and composite hydrogels did not shrink, diffusion properties are not altered. The absence of contraction can be explained by the original stiffness of the composite and pure THA hydrogels which is at least twice as high in composite hydrogels than that in pure collagen hydrogels.<sup>39,40</sup> It could also be explained by the biochemical nature of composite and pure THA hydrogels. Contraction depends on the cell/matrix interactions *via* cellular receptors. Indeed, cells need to spread and organize their cytoskeleton to contract the polymeric network.<sup>41</sup> When THA is added in a large quantity to hydrogels, the cell/matrix interactions *via* CD 44 and RHAMM receptors are weak and prevent contraction.<sup>21</sup> This is confirmed by the observation of a rounded morphology in pure THA or collagen/THA composite hydrogels, suggesting their weak interaction. The cell morphology within composite hydrogels resembles the NP cell one.<sup>42,43</sup> This was expected as natural NP cells are in a highly hydrated environment consisting of a large quantity of polysaccharides.<sup>4</sup>

THA also had an impact on cell viability. Cell adhesion was optimal for pure collagen hydrogels but decreased when the THA content increased in composite hydrogels. This shows that collagen is required to achieve optimal cell viability as it provides adequate cues to cells for adhesion and survival.<sup>23,26</sup> Cell viability in pure collagen hydrogels was constant suggesting an inhibition of cell multiplication due to the hydrogel contraction.<sup>31,44</sup> In the differentiation medium, a drop in the cell viability was observed at day 28. This could be due to an apoptotic phenomenon as previously seen for fibroblasts cultured in contracted collagen hydrogels.<sup>45</sup> In contrast, hydrogel stability and adequate biochemical cues seem to promote BM-MSCs viability. Collagen/THA composite hydrogels with 1 : 5 and 1 : 2 ratios have the same collagen content than pure collagen hydrogels but they did not contract thanks to the THA network. This allows rapid medium diffusion and cell proliferation as the porosity is great. Despite the weak interaction with their matrix, BM-MSCs proliferated within pure THA hydrogels, suggesting a remodeling of the hydrogel to increase adherence. Notably, the rheological properties of composite hydrogels did not seem to impact cell viability, as

BM-MSCs had the same metabolic activity in the 1 : 2 and 1 : 5 hydrogels despite a different stiffness.

The performance of a cellularized biomaterial to promote the Nucleus Pulposus regeneration is evaluated by the cellular production of aggrecan and collagen 2 which restore the NP hydration and its native fibrillar network. In contrast, the expression of collagen 1 has to be low as it is a marker of Annulus Fibrosus cells and osteoblast differentiation.<sup>46,47</sup> TGFβ1 is known to promote BM-MSCs differentiation into chondrocytes<sup>48</sup> whereas GDF5 favors the NP cell phenotype appearance.<sup>32</sup> In addition, these growth factors act in synergy to enhance the production of the NP extracellular matrix and NP specific markers.<sup>32</sup> The THA content had a slight effect on the gene expression of aggrecan within composite hydrogels. Besides, the differentiation medium seems to accelerate the expression of this proteoglycan without increasing its level. As aggrecan gene expression is higher in pure THA hydrogels than in composite or pure collagen hydrogels, a weak adhesion seems to be required to promote this gene expression. Collagen 2 gene expression is only detected at day 28 when cells are cultured in the proliferation medium and the THA content has a strong impact on this gene expression. BM-MSCs in pure collagen hydrogels do not express collagen 2. When TGFβ1 and GDF5 were added, the collagen 2 expression was detected from day 7 and was 10 times higher. TGFβ1 is known to trigger the collagen 2 gene expression.<sup>49,50</sup> In addition, a high THA content is also required for an optimal collagen 2 production. This was confirmed on histological sections after collagen 2 labelling. The collagen 1 gene expression was very low within all types of hydrogels, thereby evidencing the absence of differentiation into osteoblasts and fibroblasts. Despite the higher gene expression of COL1A1 in the differentiating medium, the ratio of collagen 2/collagen 1 remained very high indicating the absence of fibroblast differentiation. Lastly, the presence of THA seems to inhibit the expression of collagen 1 as this expression is lower in composites and pure THA hydrogels. Hence, the combination of TGFβ1 and GDF 5 with a high THA content, *i.e.* a high degree of hydration and weak cell/matrix interaction, seems to act in synergy to differentiate BM-MSCs into an NP like phenotype.

SOX 9 is a major marker of NP cells but is also expressed by chondrocytes.<sup>51–53</sup> SOX 9 is only expressed at day 28 in the proliferation medium, suggesting a weak differentiation. The addition of GDF5 and TGFβ1 triggers cell differentiation toward a chondrocyte-like phenotype in composite hydrogels but was higher in pure collagen hydrogels. It has been shown that the matrix stiffness is a major stimulus to trigger chondrocyte differentiation.<sup>54</sup> As pure collagen hydrogels contract, the stiffness increases during cell culture to reach around tens of kPa.<sup>55</sup> So, BM-MSCs are in an appropriate environment to differentiate into chondrocytes. The SOX 9 gene expression in pure collagen was associated with the high gene expression of collagen 10 when cells were cultured with GDF5 and TGFβ1. Hence, cells differentiated into hypertrophic chondrocytes probably due to TGFβ1.<sup>56,57</sup> This could also explain the decrease in metabolic activity observed at day 28 as hyper-

trophic chondrocytes are prone to senescence. In addition, hypertrophic chondrocytes mineralize their matrix and eventually die.<sup>58,59</sup> Hence, pure collagen hydrogels associated with GDF5 and TGF $\beta$ 1 are not adequate biomaterials to differentiate BM-MSCs into NP-like cells. It is worth noting that the collagen 10 expression was very low in composites and pure THA hydrogels, thereby evidencing the protective effect of THA. This could be due to the stability and lower mechanical properties of these hydrogels compared to pure collagen ones. It has been shown that mechanical properties around 1 kPa (storage modulus,  $G'$ ) were more suitable to trigger differentiation into NP cells. Higher mechanical properties usually lead to osteogenic differentiation.<sup>60</sup> The hypertrophic phenotype for pure collagen hydrogels did not appear when cells were cultured in the proliferation medium. Combined with a low SOX 9 expression, this confirms the weak differentiation in the proliferation medium.

To discriminate NP cells from the chondrocyte phenotype, IBSP and KRT 18 are relevant markers.<sup>53,61</sup> IBSP is a chondrocyte and osteoblast marker weakly expressed in NP cells, and it is thereby regarded as a negative marker for NP cells.<sup>61</sup> In contrast, KRT18 is a marker highly expressed by NP cells and weakly expressed by chondrocytes.<sup>61</sup> Surprisingly, IBSP was highly expressed by cells in the proliferation medium. It has been recently shown that IBSP is an aging marker of multipotent stem cells.<sup>62</sup> Hence, without gene expression of SOX 9, we can hypothesize that BM-MSCs are not differentiated until day 14 in the proliferation medium. At day 28, IBSP gene expression decreased in composite hydrogels but KRT18 was high. It suggests that the NP cell differentiation starts at day 28 in the proliferation medium. When GDF5 and TGF $\beta$ 1 were used, IBSP expression was very low in composite and pure THA hydrogels but high in pure collagen hydrogels. This shows that collagen hydrogels with high stiffness promote the hypertrophic chondrocyte phenotype, whereas a high THA content within composite hydrogels promotes the NP cell phenotype. This is confirmed at day 28 when the KRT18 gene expression became high.

Biomaterials used as a cell carrier for NP regeneration have to promote stromal cell differentiation and provide appropriate physical properties to restore the NP function. Then, they have to be remodeled into a neo tissue by cells. Hydration is the most important physical property required to treat NP degeneration as it is responsible for the restoration of the disc height. For this reason, highly hydrated hydrogels were used in the first place. Synthetic polymers such as PEG or pNIPAM are interesting as they are easy to synthesize and their physical properties can be tuned to mimic the NP ones.<sup>15,16</sup> In addition, some of them are biologically active and promote BM-MSC differentiation into NP cells.<sup>15</sup> However, they are not degraded by cells.<sup>63</sup> Therefore, their remodeling is not controllable. Natural biopolymers from marine organisms such as agarose or alginate have the same drawbacks.<sup>16</sup> That's the reason why collagen and hyaluronic acid were chosen to synthesize biomimetic hydrogels in this study because they are degradable and allow for biomaterial remodeling. The major

drawback of collagen/HA hydrogels is their poor mechanical properties despite their higher performance compared to fibrin hydrogels.<sup>64</sup> To achieve NP physical properties, they have to be cross-linked.<sup>4</sup> Cross-linkers such as EDC or glutaraldehyde can be harmful and decrease hydrogel degradation.<sup>4,34</sup> In addition, mixing collagen and HA with cross-linkers leads to materials without collagen fibrils. Hence, the NP topography is lost. Using enzymatic cross-linking *via* HRP, cell survival was favored in biomimetic collagen/THA hydrogels due to the mild conditions.<sup>26</sup> Hence, we restored the topographical feature of NP, even though collagen II was not used. Usually, research performed on collagen/HA hydrogels focuses on a unique formulation and often uses a low HA content to prevent the formation of polyionic complexes.<sup>34</sup> The appropriate quantity of both biopolymers to reach a high degree of hydration and cell differentiation is not studied. Here, we performed a systematic study to find that a high content of THA and the addition of discogenic factors are required to promote such differentiation. Besides, collagen is essential to achieve high cell viability. In addition, enzymatic crosslinking allows for remodeling by cellular enzymes as previously shown.<sup>26</sup> We found the compromise between hydration, cell adhesion, mechanical properties and the ability to promote cell differentiation to generate a biomaterial suitable for NP regeneration.

## 5. Conclusions

This study shows that the combination of a high THA content with discogenic growth factors is required to promote the differentiation of BM-MSCs into NP-like cells within collagen/THA composite hydrogels. Hydrogel stability and mechanical properties around 500 Pa are strong stimuli for long term cell viability, whereas collagen ensures cell adhesion and short-term survival. A high THA level impacts cell/matrix interactions and increases the degree of hydration to direct the cell morphology and phenotype toward the NP cell phenotype. Using a 1 : 5 collagen/THA ratio, similar to that in NP, the cells adopt the characteristic rounded morphology and highly expressed the specific NP extracellular matrix biopolymers *i.e.* aggrecan and collagen 2. In contrast, pure collagen hydrogels are not adequate for NP regeneration as cells differentiated into hypertrophic chondrocytes. Hence, injectable and biomimetic hydrogels with a high degree of hydration (owing to a high THA content) with a small proportion of fibrillar collagen seem to be promising biomaterials for NP regeneration.

## Conflicts of interest

There are no conflicts of interest to declare.

## Acknowledgements

This project has been supported by "L'Agence Nationale de la Recherche" (ANR) and the Swiss National Science Foundation

(SNSF): INDEED project, SNSF's grant number 310030E\_189310 and ANR's grant number ANR-19-CE06-0028. We thank Dr Francisco Fernandes for his helpful advice.

## References

- G. B. D. Disease, I. Injury and C. Prevalence, *Lancet*, 2018, **392**, 1789–1858.
- J. N. Katz, *J. Bone Jt. Surg., Am. Vol.*, 2006, **88**(Suppl 2), 21–24.
- C. L. Le Maitre, A. Pockert, D. J. Buttle, A. J. Freemont and J. A. Hoyland, *Biochem. Soc. Trans.*, 2007, **35**, 652–655.
- R. D. Bowles and L. A. Setton, *Biomaterials*, 2017, **129**, 54–67.
- J. Silva-Correia, S. I. Correia, J. M. Oliveira and R. L. Reis, *Biotechnol. Adv.*, 2013, **31**, 1514–1531.
- J. P. Urban and C. P. Winlove, *J. Magn. Reson. Imaging*, 2007, **25**, 419–432.
- C. V. Maldonado, R. D. Paz and C. B. Martin, *Eur. Spine J.*, 2011, **20**(Suppl 3), 403–407.
- J. E. Zigler, J. Glenn and R. B. Delamarter, *J. Neurosurg.*, 2012, **17**, 504–511.
- J. Clouet, M. Fusellier, A. Camus, C. Le Visage and J. Guicheux, *Adv. Drug Delivery Rev.*, 2019, **146**, 306–324.
- G. Vadala, G. Sowa, M. Hubert, L. G. Gilbertson, V. Denaro and J. D. Kang, *J. Tissue Eng. Regener. Med.*, 2012, **6**, 348–355.
- Y. Peng, D. Huang, S. Liu, J. Li, X. Qing and Z. Shao, *Front. Bioeng. Biotechnol.*, 2020, **8**, 56.
- D. Sakai, J. Mochida, T. Iwashina, A. Hiyama, H. Omi, M. Imai, T. Nakai, K. Ando and T. Hotta, *Biomaterials*, 2006, **27**, 335–345.
- M. Peroglio, D. Eglin, L. M. Benneker, M. Alini and S. Grad, *Spine J.*, 2013, **13**, 1627–1639.
- K. Zheng and D. Du, *J. Tissue Eng. Regener. Med.*, 2021, **15**, 299–321.
- A. A. Thorpe, V. L. Boyes, C. Sammon and C. L. Le Maitre, *Acta Biomater.*, 2016, **36**, 99–111.
- T. C. Schmitz, E. Salzer, J. F. Crispim, G. T. Fabra, C. LeVisage, A. Pandit, M. Tryfonidou, C. L. Maitre and K. Ito, *Acta Biomater.*, 2020, **114**, 1–15.
- B. Reid, M. Gibson, A. Singh, J. Taube, C. Furlong, M. Murcia and J. Elisseeff, *J. Tissue Eng. Regener. Med.*, 2015, **9**, 315–318.
- D. R. Pereira, J. Silva-Correia, J. M. Oliveira and R. L. Reis, *J. Tissue Eng. Regener. Med.*, 2013, **7**, 85–98.
- D. Sakai, J. Mochida, Y. Yamamoto, T. Nomura, M. Okuma, K. Nishimura, T. Nakai, K. Ando and T. Hotta, *Biomaterials*, 2003, **24**, 3531–3541.
- A. Sorushanova, L. M. Delgado, Z. Wu, N. Shologu, A. Kshirsagar, R. Raghunath, A. M. Mullen, Y. Bayon, A. Pandit, M. Raghunath and D. I. Zeugolis, *Adv. Mater.*, 2019, **31**, e1801651.
- X. Xu, A. K. Jha, D. A. Harrington, M. C. Farach-Carson and X. Jia, *Soft Matter*, 2012, **8**, 3280–3294.
- J. Lam, N. F. Truong and T. Segura, *Acta Biomater.*, 2014, **10**, 1571–1580.
- C. Loebel, S. E. Szczesny, B. D. Cosgrove, M. Alini, M. Zenobi-Wong, R. L. Mauck and D. Eglin, *Biomacromolecules*, 2017, **18**, 855–864.
- S. Chen, Q. Zhang, T. Nakamoto, N. Kawazoe and G. Chen, *J. Mater. Chem. B*, 2014, **2**, 5612–5619.
- Q. Xu, J. E. Torres, M. Hakim, P. M. Babiak, P. Pal, C. M. Battistoni, M. Nguyen, A. Panitch, L. Solorio and J. C. Liu, *Mater. Sci. Eng., R*, 2021, **146**, 100641.
- A. Frayssinet, D. Petta, C. Illoul, B. Haye, A. Markitantova, D. Eglin, G. Mosser, M. D'Este and C. Helary, *Carbohydr. Polym.*, 2020, **236**, 116042.
- M. Camman, P. Joanne, J. Brun, A. Marcellan, J. Dumont, O. Agbulut and C. Helary, *Biomater. Adv.*, 2023, **144**, 213219.
- D. W. Bannister and A. B. Burns, *Analyst*, 1970, **95**, 596–600.
- C. Loebel, T. Stauber, M. D'Este, M. Alini, M. Zenobi-Wong and D. Eglin, *J. Mater. Chem. B*, 2017, **5**, 2355–2363.
- M. W. Pfaffl, *Nucleic Acids Res.*, 2001, **29**, e45.
- C. Helary, I. Bataille, A. Abed, C. Illoul, A. Anglo, L. Louedec, D. Letourneur, A. Meddahi-Pelle and M. M. Giraud-Guille, *Biomaterials*, 2010, **31**, 481–490.
- P. Colombier, J. Clouet, C. Boyer, M. Ruel, G. Bonin, J. Lesoeur, A. Moreau, B. H. Fellah, P. Weiss, L. Lescaudron, A. Camus and J. Guicheux, *Stem Cells*, 2016, **34**, 653–667.
- B. Gantenbein-Ritter, L. M. Benneker, M. Alini and S. Grad, *Eur. Spine J.*, 2011, **20**, 962–971.
- L. Calderon, E. Collin, D. Velasco-Bayon, M. Murphy, D. O'Halloran and A. Pandit, *Eur. Cells Mater.*, 2010, **20**, 134–148.
- D. M. Aladin, K. M. Cheung, A. H. Ngan, D. Chan, V. Y. Leung, C. T. Lim, K. D. Luk and W. W. Lu, *J. Orthop. Res.*, 2010, **28**, 497–502.
- X. Cun and L. Hosta-Rigau, *Nanomaterials*, 2020, **10**, 2070.
- S. A. Hilton, L. C. Dewberry, M. M. Hodges, J. Hu, J. Xu, K. W. Liechty and C. Zgheib, *PLoS One*, 2019, **14**, e0218536.
- F. Lee, J. E. Chung and M. Kurisawa, *Soft Matter*, 2008, **4**, 880–887.
- E. E. Antoine, P. P. Vlachos and M. N. Rylander, *Tissue Eng., Part B*, 2014, **20**, 683–696.
- H. F. Chieh, Y. Sun, J. D. Liao, F. C. Su, C. Zhao, P. C. Amadio and K. N. An, *J. Biomed. Mater. Res., Part A*, 2010, **93**, 1132–1139.
- S. Kasugai and H. Ogura, *Arch. Oral Biol.*, 1993, **38**, 785–792.
- W. E. Johnson and S. Roberts, *J. Anat.*, 2003, **203**, 605–612.
- N. Vanawati, A. Barlian, H. Judawisastra and I. Wibowo, *Future Sci. OA*, 2022, **8**, FSO810.
- A. W. Lund, B. Yener, J. P. Stegemann and G. E. Plopper, *Tissue Eng., Part B*, 2009, **15**, 371–380.
- C. Helary, M. Zarka and M. M. Giraud-Guille, *J. Tissue Eng. Regener. Med.*, 2012, **6**, 225–237.

- 46 O. M. Torre, V. Mroz, M. K. Bartelstein, A. H. Huang and J. C. Iatridis, *Ann. N. Y. Acad. Sci.*, 2019, **1442**, 61–78.
- 47 E. Wrobel, J. Leszczynska and E. Brzoska, *Cell. Mol. Biol. Lett.*, 2016, **21**, 26.
- 48 R. Tuli, S. Tuli, S. Nandi, X. Huang, P. A. Manner, W. J. Hozack, K. G. Danielson, D. J. Hall and R. S. Tuan, *J. Biol. Chem.*, 2003, **278**, 41227–41236.
- 49 I. Grafe, S. Alexander, J. R. Peterson, T. N. Snider, B. Levi, B. Lee and Y. Mishina, *Cold Spring Harbor Perspect. Biol.*, 2018, **10**, a022202.
- 50 H. S. Hwang, M. H. Lee and H. A. Kim, *FASEB J.*, 2020, **34**, 9531–9546.
- 51 X. Jiang, X. Huang, T. Jiang, L. Zheng, J. Zhao and X. Zhang, *Biomater. Sci.*, 2018, **6**, 1556–1568.
- 52 U. Noth, L. Rackwitz, A. Heymer, M. Weber, B. Baumann, A. Steinert, N. Schutze, F. Jakob and J. Eulert, *J. Biomed. Mater. Res., Part A*, 2007, **83**, 626–635.
- 53 M. V. Risbud, Z. R. Schoepflin, F. Mwale, R. A. Kandel, S. Grad, J. C. Iatridis, D. Sakai and J. A. Hoyland, *J. Orthop. Res.*, 2015, **33**, 283–293.
- 54 Y. Zhou, J. Qiu, L. Wan and J. Li, *J. Mol. Histol.*, 2022, **53**, 805–816.
- 55 Z. Feng, M. Yamato, T. Akutsu, T. Nakamura, T. Okano and M. Umezū, *Artif. Organs*, 2003, **27**, 84–91.
- 56 F. Barry, R. E. Boynton, B. Liu and J. M. Murphy, *Exp. Cell Res.*, 2001, **268**, 189–200.
- 57 K. Futrega, P. G. Robey, T. J. Klein, R. W. Crawford and M. R. Doran, *Commun. Biol.*, 2021, **4**, 29.
- 58 Y. A. Ahmed, L. Tatarczuch, C. N. Pagel, H. M. Davies, M. Mirams and E. J. Mackie, *Osteoarthr. Cartil.*, 2007, **15**, 575–586.
- 59 M. R. Coe, T. A. Summers, S. J. Parsons, A. L. Boskey and G. Balian, *Bone Miner.*, 1992, **18**, 91–106.
- 60 Y. Navaro, N. Bleich-Kimelman, L. Hazanov, I. Mironi-Harpaz, Y. Shachaf, S. Garty, Y. Smith, G. Pelled, D. Gazit, D. Seliktar and Z. Gazit, *Biomaterials*, 2015, **49**, 68–76.
- 61 R. Rodrigues-Pinto, S. M. Richardson and J. A. Hoyland, *Bone Joint Res.*, 2013, **2**, 169–178.
- 62 I. H. Bellayr, J. G. Catalano, S. Lababidi, A. X. Yang, J. L. Lo Surdo, S. R. Bauer and R. K. Puri, *Stem Cell Res. Ther.*, 2014, **5**, 59.
- 63 Z. Cui, B. H. Lee, C. Pauken and B. L. Vernon, *J. Biomed. Mater. Res., Part A*, 2011, **98**, 159–166.
- 64 J. Gansau and C. T. Buckley, *J. Funct. Biomater.*, 2018, **9**, 43.